THE JOURNAL OF BIOLOGICAL CHEMISTRY
Vol. 274, No. 6, Issue of February 5, pp. 3667–3671, 1999

Printed in U.S.A.

Kinesin Takes One 8-nm Step for Each ATP That It Hydrolyzes*

(Received for publication, August 27, 1998, and in revised form, November 5, 1998)

David L. Coy‡, Michael Wagenbach, and Jonathon Howard§

From the Department of Physiology and Biophysics, University of Washington, Seattle, Washington 98195-7290

Conventional kinesin is a motor protein that moves stepwise along microtubules carrying membrane-bound organelles toward the periphery of cells. The steps are of amplitude 8.1 nm, the distance between adjacent tubulin binding sites, and are powered by the hydrolysis of ATP. We have asked: how many steps does kinesin take for each molecule of ATP that it hydrolyzes? To answer this question, the motility and ATP hydrolysis of recombinant, heterotetrameric and homodimeric conventional *Drosophila* kinesins adsorbed to 200-nm-diameter casein-coated silica beads were assayed under identical, single-molecule conditions. Division of the speed by the maximum microtubule-activated ATPase rate gave a stoichiometry of 1.08 ± 0.09 steps for each ATP hydrolyzed at 1 mM ATP. Therefore, under low loads in which the drag force ≪ 1 pN, coupling between the chemical and mechanical cycles of kinesin is tight, consistent with conventional power stroke models. Our results rule out models that require two or more ATPs/step, such as some thermal ratchet models, or that propose multiple steps powered by single ATPs.

Conventional kinesin is a protein machine that steps along the surface of a microtubule as it carries a membrane-bound organelle toward the periphery of a cell (1–3). The size of the steps is ~8 nm (4, 5). This is the distance between consecutive binding sites along the microtubule protofilament (6, 7), and a single kinesin molecule can take hundreds of steps without detaching (8, 9), even against opposing loads as high as ~6 pN (10–12). The steps are driven by the hydrolysis of ATP; kinesin is an ATPase (13) whose speed of movement increases linearly with ATP concentration until it approaches a maximum of about 800 nm/s (8, 14), and AMP-PNP,[1] a nonhydrolyzable analog of ATP, arrests movement (15, 16). Despite intensive biochemical, biophysical, and structural investigations over the last few years, there remains considerable uncertainty as to the mechanism by which the stepping is coupled to ATP hydrolysis.

In this work, we address the question: what is the stoichiometry of kinesin? In other words, how many steps does kinesin take for each ATP that it hydrolyzes? This question is important because it tests different models proposed to explain how motor proteins such as kinesin and myosin work. For example, one class of "thermal ratchet" models predicts that the stoichiometry is ≤0.5 steps/ATP (17, 18); these models postulate that ATP hydrolysis rectifies a diffusive motion in such a way that a step only occurs if the diffusion is *toward* the next binding site. Because there is an equal probability that the motor diffuses away from the next binding site (*i.e.* in the wrong direction), this model predicts that on average at least two molecules of ATP are hydrolyzed per forward step. A stoichiometry of less than one could also be due to "futile" hydrolysis cycles, those that fail to produce steps and lead to "slippage" between the mechanical and chemical cycles. Other models postulate a stoichiometry greater than 1 and have been applied to reconcile the high efficiency of muscle with the mechanical properties of muscle fibers (19, 20) or to reconcile the large apparent "interaction distance" between myosin and actin with the smaller physical size of the myosin head (21, 22). However, there are alternative explanations of these results that do not require more than one step/ATP hydrolysis (23). On the middle ground are conventional "tightly coupled" models in which the mechanical and chemical cycles are assumed to be strictly coordinated, predicting a stoichiometry of 1.

Some clues to the mechanochemical stoichiometry of kinesin have already been obtained. High resolution tracking experiments show that one ATP produces no more than one step, because bursts of multiple 8-nm steps are not observed at limiting, low ATP concentrations (5, 14, 24). On the other hand, the linear relationship between speed and ATP concentration (at low ATP concentration) indicates that one ATP is sufficient to produce a step (8); if two (or more) ATPs were required, then the speed would depend on the square (or a higher power) of the ATP concentration. This conclusion is supported by tracking experiments at low ATP concentration showing that time intervals between steps are exponentially distributed (5, 14); if two (or more) ATPs were required, the interval distribution would be peaked rather than monotonically decreasing. These results are consistent with a stoichiometry of 1 but do not prove it. For example, the latter results imply that the binding of one ATP molecule can result in a step, but they provide no information about the likelihood that a step will actually occur. Thus these experiments do not measure the stoichiometry.

In this work, we measure the stoichiometry of kinesin by comparing its rate of ATP hydrolysis to its rate of stepping. Under conditions in which a single kinesin molecule is moving along a microtubule, division of the speed of movement (v) by the maximal, microtubule-stimulated ATPase rate/molecule (k_{cat}) yields the *fuel economy* of the motor (the distance/ATP hydrolyzed). Division of the economy by the step size, d = 8.1 nm (25), then yields the number of steps/ATP hydrolyzed, *i.e.* the stoichiometry (n) as shown.

$$n = \frac{v}{d \cdot k_{cat}} \quad \text{(Eq. 1)}$$

* This work was supported by National Institutes of Health Grant AR40593 and by a grant from the Human Frontier Science Program (to J. H.). The costs of publication of this article were defrayed in part by the payment of page charges. This article must therefore be hereby marked "*advertisement*" in accordance with 18 U.S.C. Section 1734 solely to indicate this fact.

The nucleotide sequence(s) reported in this paper has been submitted to the GenBank™/EBI Data Bank with accession number(s) AF053733 and AF055298.

‡ Supported by National Institutes of Health Molecular Biophysics Training Grant GM08268 and by the Achievement Reward for College Scientists Foundation.

§ To whom correspondence should be addressed: Dept. of Physiology & Biophysics, University of Washington, Box 357290, Seattle, WA 98195-7290. Fax: 206-685-0619; E-mail: johoward@u.washington.edu.

[1] The abbreviations used are: AMP-PNP, adenosine 5′-(β,γ-imino)-triphosphate; GMP-CPP, guanylyl-(α,β)-methylene-diphosphonate; PIPES, 1,4-piperazinediethanesulfonic acid.

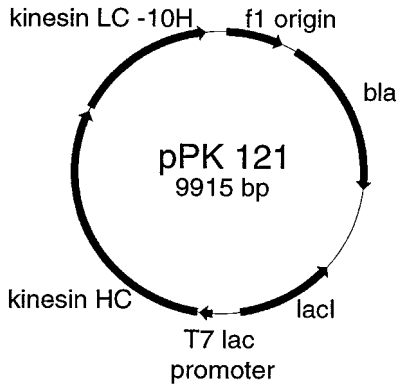

FIG. 1. **Plasmid diagram of pPK121; co-expression of heterotetrameric ($\alpha_2\beta_2$) conventional *Drosophila* kinesin from pET21a+.**

Until now, kinesin ATPase assays have been typically done with molecules in solution, whereas motility assays have been done with the motors bound to a solid support (*e.g.* to a glass surface or bead). This has resulted in apparent stoichiometries varying from as high as 200 for native, full-length *Drosophila* kinesin (v = 900 nm/s, k_{cat} = 0.60 s^{-1}; Ref. 26) to as low as 0.008 for a recombinant, *Drosophila* kinesin motor domain-glutathione *S*-transferase fusion protein (v = 1.5 nm/s, k_{cat} = 24 s^{-1}; Ref. 27). This 25,000-fold range of stoichiometries, together with an inverse correlation between speed and ATPase rate, suggests that binding of kinesin to a solid support may have profound effects on the speed and/or ATPase. For this reason, we have measured the ATP hydrolysis rate of kinesin under identical conditions to those used to assay the motility, namely with kinesin bound to 200-nm-diameter silica beads. At low kinesin-to-bead ratios where the motility is due to single motors, the stoichiometry is unity.

EXPERIMENTAL PROCEDURES

Preparation of pPK121 and pPK113 Kinesin Constructs—Two kinesin expression plasmids were constructed in pET vectors. One plasmid (pPK113) contained a histidine-tagged conventional kinesin heavy chain. The second plasmid (pPK121; Fig. 1) was designed for co-expression of the kinesin heavy chain with histidine-tagged light chains. All enzymes were purchased from New England BioLabs (Beverly, MA), except T4 DNA ligase (Life Technologies, Inc.) and T4 gene 32 protein (Boehringer Mannheim). DNA propagation steps were performed in *Escherichia coli* DH5α or CJ236.

Plasmids containing a modified *Drosophila melanogaster* kinesin heavy chain gene (pET-Kin) and the *D. melanogaster* kinesin light chain gene (pBS-13a) were a gift from L. Goldstein. The heavy chain gene was modified by polymerase chain reaction and oligo-directed mutagenesis to restore the wild type N-terminal amino acid sequence, introduce silent mutations for subsequent handling, and reduce predicted RNA secondary structure. For the pPK113 plasmid, the heavy chain gene was additionally modified by polymerase chain reaction to introduce a C-terminal hexahistidine and thrombin cleavage sequence (LVPRGS) tag. The genes were cloned into pET20b+ (Novagen, Milwaukee, WI), and both strands of the final heavy chain constructs were sequenced to verify the predicted translation products.

The light chain gene was modified by polymerase chain reaction to add a C-terminal decahistidine tag, and silent mutations were introduced at the 5′ end of the gene to reduce predicted RNA secondary structure and to avoid low frequency codons. The modified light chain gene and a heavy chain gene were co-expressed from a pET21a+ plasmid (Novagen). The complete sequences of our pPK113 and pPK121 expression plasmids have been deposited in the GenBank data base (accession numbers AF053733 and AF055298, respectively).

Kinesin Expression—Both kinesin constructs were expressed in *E. coli* BL21(DE3)[pLysS]. Cultures grown in LB at 37 °C to an optical density of 1 at 600 nm (Hewlett-Packard 8452 Diode Array Spectrophotometer, Fullerton, CA) were induced with 0.4 mM isopropyl-β-D-thiogalactopyranoside at 20 °C for 3–4 h. Unless otherwise noted, all buffers were augmented with 50–100 μM MgATP. The bacterial cells were harvested and resuspended in ~30 ml of lysis buffer (50 mM sodium phosphate, 300 mM NaCl, 40 mM imidazole, 5 mM 2-mercaptoethanol, 10% glycerol, pH 8.0)/liter of culture, lysed in a French press at ~19,000 psi, sonicated, and centrifuged (100,000 × g) for 30 min at 4 °C.

Purification of Recombinant, Full-length Kinesin with Light Chains—Heterotetrameric kinesin, consisting of both heavy and light chains, was purified in two steps using nickel-nitrilotriacetic acid agarose and phosphocellulose resins. The tagged light chains and associated heavy chains were purified from other bacterial proteins by batch absorption to nickel-nitrilotriacetic acid agarose resin (Qiagen, Valencia, CA). The resin was poured into a column and washed with wash buffer (50 mM sodium phosphate, pH 7.0, 1 M NaCl, 5 mM 2-mercaptoethanol, and 80 mM imidazole), and eluted with elution buffer (50 mM sodium phosphate, pH 7.0, 300 mM NaCl, 5 mM 2-mercaptoethanol, and 500 mM imidazole). The eluate contained a large excess of light chain relative to the amount of heavy chain. To isolate tetrameric kinesin from excess light chains, the mixture was changed into PC buffer (50 mM sodium phosphate, pH 7.0, 100 mM NaCl, 4 mM $MgCl_2$, 2 mM EDTA, 1 mM 2-mercaptoethanol, 1% glycerol) by dialysis at 4 °C and passed over a column of P-11 phosphocellulose (Whatman, Hillsboro, OR). The phosphocellulose has low affinity for light chains; light chains not bound to a heavy chain pass through the column without being retained. Kinesin was then eluted with a linear sodium chloride gradient (0.1–1 M) in PC buffer. The peak fractions were combined, dialyzed into storage buffer (50 mM imidazole, pH 7.0, 100 mM NaCl, 1 mM $MgCl_2$, 2 mM EGTA, 0.1 mM EDTA, 5% (w/v) sucrose, 5 mM 2-mercaptoethanol) with 1.0 μM MgATP, frozen in liquid nitrogen, and stored at −80 °C. The homodimeric construct consisting of only the kinesin heavy chains was purified in a similar manner.

Coomassie-stained SDS-polyacrylamide gels were scanned (Umax PS-2400X, Umax Data Systems, Hsinchu, Taiwan) and analyzed with NIH Image version 1.57 for Apple Macintosh. The molar ratio of light chain to heavy chain, based on relative dye staining, ranged from 1.2 to 1.5 in three independent preparations. Sucrose density centrifugation in storage buffer, which has a similar ionic strength to BRB80, was consistent with a heterotetrameric protein of sedimentation coefficient 8.7 ± 0.3 S ($\alpha_2\beta_2$; data not shown), similar to the sedimentation coefficient of heterotetrameric bovine brain kinesin in its folded conformation (28). Initial characterization of the recombinant wild type protein in standard microtubule gliding assays resulted in gliding speeds that were similar to native bovine brain kinesin.

Preparation of Casein-coated Silica Beads and Kinesin Adsorption—A stock solution of 2 nM 0.2-μm-diameter silica beads (Bangs Laboratories, Carmel, IN) and 2 mg/ml casein was bath sonicated for 3–4 h to disperse the beads and stored at 4 °C. The solution was stable over several days. The recombinant kinesin was adsorbed to the casein-coated beads by mixing the two together rapidly, vortexing, and incubating for 10 min. Adsorption to the beads was confirmed by Western blot with SUK4 monoclonal antibody (data not shown).

Radiometric Determination of Kinesin Concentration—The concentration of active kinesin was determined as half the concentration of nucleotide binding sites, because there are two ATP binding sites/molecule. The number of nucleotide binding sites was measured radiometrically as follows. BA85 nitrocellulose membranes (Schleicher & Schuell) were prepared by washing in 0.4 N KOH for 10 min, rinsing in double distilled H_2O, and incubating in cold BRB80 buffer (80 mM potassium PIPES, pH 6.9, 1 mM EGTA, 1 mM $MgCl_2$) for at least 1 h prior to use. The exchange reactions were run in BRB80 buffer augmented with 1 mg/ml casein, 1 mM $MgCl_2$, and 250 nM [α-^{32}P]ATP (NEN Life Science Products) for 1–2 h at room temperature. A small aliquot (3 μl) was placed on the 25-mm circular nitrocellulose membrane (held on a filter support under vacuum), and the membrane was washed with 500 μl of cold BRB80. The membrane was then dried at 60 °C, combined with scintillation mixture, and read in a Beckman scintillation counter. The reading was then compared with a standard curve constructed by diluting the reaction mixture into BRB80 + 1 mg/ml casein and dotting directly onto the membranes with no wash.

The concentration of kinesin was measured for the enzyme in solution in the absence of beads. Adsorbing kinesin to beads had no significant effect on the amount of nucleotide that it binds: the nucleotide binding activity of kinesin on beads was 120 ± 18% that of kinesin in solution. Therefore, adsorbing kinesin to the casein-coated silica beads does not cause an appreciable amount of denaturation of the protein. However, there remains the possibility that some of the kinesin molecules adsorbed to beads may not be able to access microtubules, even though they can still bind nucleotide. For example, suppose that half the motors adsorb "heads-up" (*i.e.* able to bind to and move along microtubules) and half adsorb "heads-down" (*i.e.* unable to bind to or move along microtubules but still able to bind nucleotide). Then the microtubule-stimulated ATPase rate/motile kinesin would be underestimated by a factor of 2. To rule out this possibility, heterotetrameric kinesin was adsorbed to the casein-coated silica beads and loaded with [α-^{32}P]ATP on ice. The labeled nucleotide was then chased by diluting the kinesin mixture into buffer (0 °C) containing 1 mM MgATP in the

presence and absence of 5 μM microtubules polymerized in the presence of GMP-CPP (to prevent cold-induced depolymerization; Ref. 29). In the presence of microtubules, 86 ± 4% (S.E.) of the radionucleotide was released within 1 min, the resolution of the assay. This indicates that most bead-adsorbed kinesin was accessible to microtubules. We did not correct the kinesin concentration for these relatively small effects of the beads on the effective kinesin concentration.

Microtubules—Microtubules were polymerized from bovine brain tubulin at 37 °C in BRB80 with 4 mM $MgCl_2$, 1 mM GTP and 5% (v/v) Me_2SO. The microtubules were stabilized with 10 μM taxol, airfuged at 28 psi in a Beckman airfuge through a cushion of 1:1 BRB80:glycerol with 10 μM taxol to remove excess guanosine nucleotide, resuspended in BRB80 with 10 μM taxol, and thrice sheared through a 30-gauge needle. The concentration of tubulin was determined by absorbance at 276 nm in 6 M guanidine HCl using an extinction coefficient of 1.03 ml/mg·cm. Microtubule concentrations are expressed in terms of 100-kDa tubulin heterodimers.

In Vitro Motility Assays—The speed of kinesin adsorbed to 200-nm casein-coated silica beads was measured in motility assays. Standard flow cells were constructed (30) using coverslips that had been treated with 3-aminopropyl triethoxysilane (Pierce) to attach microtubules to the surface. The treatment consisted of washing coverslips with 2% PCC-54 detergent and rinsing with distilled water. After drying, the coverslips were soaked in a 20% solution of 3-aminopropyl triethoxysilane in acetone for 5 min followed by short rinses with acetone and with distilled water. The coverslips were then rinsed for 15 min in slow flowing distilled water and air-dried.

A microtubule solution containing ~3 μM tubulin was incubated in the flow cell for 15 min. The chamber was then washed with several changes of motility buffer (BRB80 + 10 μM taxol, 20 mM D-glucose, 20 μg/ml glucose oxidase, 8 μg/ml catalase, 0.5% 2-mercaptoethanol, 1 mM MgATP) after which a solution of kinesin adsorbed to beads diluted in motility buffer was introduced. Beads and microtubules were visualized by differential interference contrast microscopy on an inverted microscope (Zeiss Axiovert), the video images were taken with a Hamamatsu C2400 CCD camera and control unit, and the data were stored on videotape with a Panasonic AG7350 VCR (Proline, Kirkland, WA) for subsequent analysis. The speed was determined by dividing the total distance that the bead moved along a microtubule by the duration of movement.

ATPase Measurements—Steady-state ATPase rate was measured in BRB80 with 1 mM MgATP, 10 μM taxol, 1 mg/ml casein, and a variable amount of taxol-stabilized microtubules. The mixtures were incubated at 25 °C, and the reaction was halted by adding an equal volume of cold 1 N perchloric acid + 0.2% Triton X-100. The samples were vortexed and centrifuged (18,000 × *g*) to remove precipitated proteins. The phosphate concentration was determined by adding malachite green solution (3 g of sodium molybdate, 0.25 g of malachite green oxalate, and 0.25 g of Triton X-100/liter 0.7 N HCl) and reacting for 1 min. The colorimetric reaction was quenched by the addition of 1.4 N sulfuric acid, and the absorbance at 640 nm was read and compared against a phosphate calibration. In parallel with each sample, a control was run in which the kinesin was added after the PCA quench. The difference in phosphate concentration between the sample and control represents the phosphate liberated by kinesin. This was divided by the product of the incubation time and one-half the concentration of nucleotide binding sites (2 ATP binding sites/kinesin molecule); the turnovers are therefore expressed per kinesin molecule. The enzyme was stable in our assays for greater than 4 h at room temperature.

Data were fitted to the Michaelis-Menten equation using Igor (Wavemetrics, Lake Oswego, OR) to obtain the maximal microtubule-stimulated turnover (k_{cat}) and the Michaelis constant (K_m) defined as the microtubule concentration necessary for half-maximal activation. The logarithm of the raw ATP hydrolysis measurements (kinesin + background) was taken prior to least squares curve fitting; because the relative error in each of the measurements is approximately the same for each raw data point, fitting to the logged data ensures that all the points are weighted according to their uncertainty.

RESULTS

To measure the stoichiometry of kinesin, the motility and ATP hydrolysis of recombinant, heterotetrameric and homodimeric conventional *Drosophila* kinesin adsorbed to 200-nm-diameter casein-coated silica beads were assayed under identical, single-molecule conditions. Data from three kinesin preparations are summarized in Table I.

Bead Motility—The movement of the kinesin-coated beads along microtubules adsorbed to the silanized surface of the experimental chamber was observed by differential interference contrast microscopy (Fig. 2*a*). At the resolution of the video images, the motion was smooth with fewer than 1% of the beads stopping or pausing for greater than 0.5 s. The distance traveled during each run of a bead along a microtubule varied greatly from bead to bead, even at the same kinesin-bead ratio (Fig. 2*b*). At kinesin-bead ratios of less than one, the distances were approximately exponentially distributed, consistent with detachment being a random (Poisson) process. At the lowest kinesin-bead ratio, 0.088 kinesins/bead, fewer than 10% of those beads with motors on them have more than one motor;

TABLE I
Kinesin stoichiometry

Speed and ATPase rates of single kinesin molecules attached to silica beads at 25 °C. Data from two kinesin preparations with light chains ($\alpha_2\beta_2$) and one preparation without light chains (α_2). The stoichiometry was calculated by dividing the distance per ATP by the step size (8.1 nm) and multiplying by 0.97 to correct for the effect of ADP build-up on the ATPase (see text). The uncertainties were calculated by adding the variances associated with the speed, ATPase, concentration (S.E./mean = 0.05), temperature in motility assay (S.E./mean = 0.04, corresponding to S.E. in the temperature of 0.5 °C), and temperature in the ATPase assay (S.E./mean = 0.04).

Preparation	Speed ± S.E. (v)	ATPase ± S.E. (k_{cat})	Distance/ATP	Stoichiometry (n)
	nm/s	s^{-1}	*nm/ATP*	
$\alpha_2\beta_2$	882 ± 14	94 ± 13	9.4 ± 1.3	1.12 ± 0.18
$\alpha_2\beta_2$	801 ± 18	81 ± 15	9.9 ± 1.9	1.18 ± 0.24
α_2	772 ± 29	88 ± 6	8.7 ± 0.7	1.04 ± 0.11

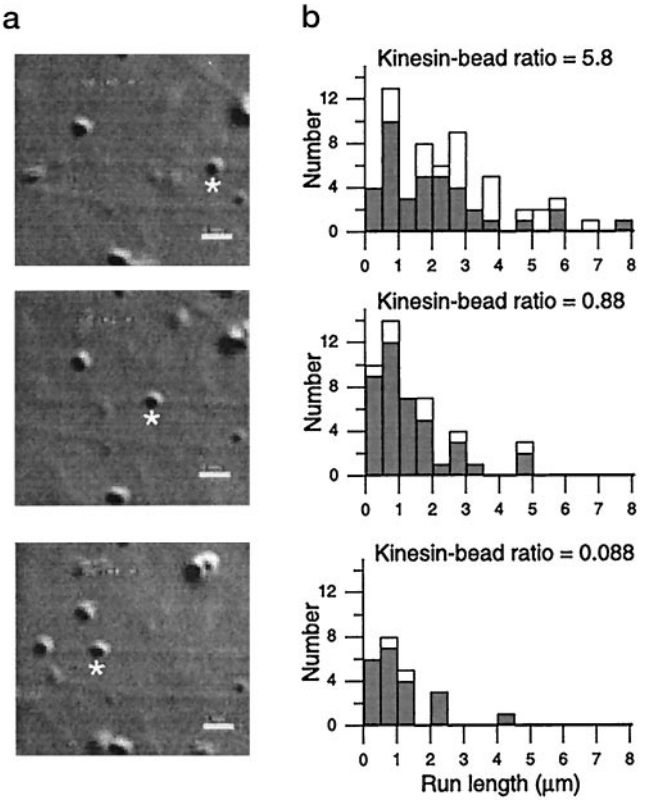

FIG. 2. **Movement along microtubules of 200-nm-diameter silica beads coated with heterotetrameric kinesin ($\alpha_2\beta_2$).** *a*, movement of a bead (*asterisk*) along a microtubule (*horizontal shadow*) at 2-s intervals. The kinesin-bead ratio was 5.8. *Scale bar* is 1 μm. *b*, histogram of bead run lengths at three kinesin-bead ratios. The *dark bars* correspond to beads that detached before reaching the end of the microtubule. The *light bars* correspond to the other beads and include those whose detachment was not observed because they moved off the screen.

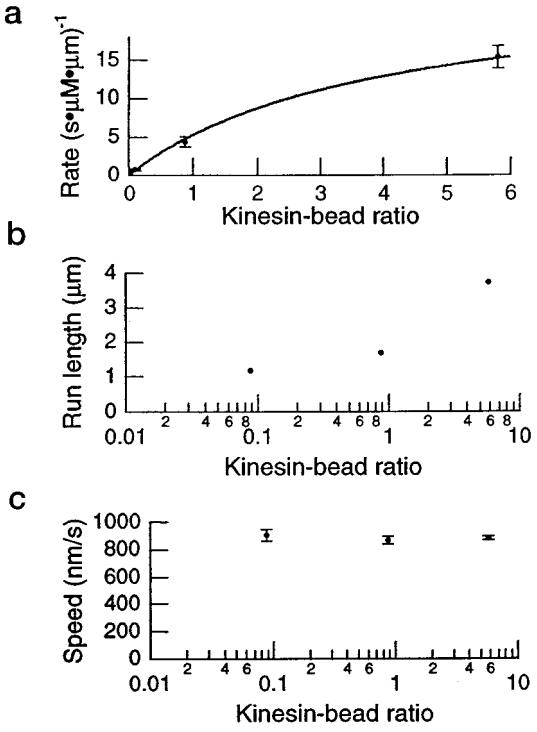

FIG. 3. **Attachment, movement, and speed of kinesin-coated beads on microtubules.** All data were from the same $\alpha_2\beta_2$ kinesin preparation as Fig. 2 (1 mM ATP). *a*, the rate of bead attachment to microtubules as a function of the average kinesin-bead ratio. The *line* is a Michaelis-Menten fit with k_{cat} of 25 s^{-1} $\mu M^{-1}/\mu m$ microtubule and K_m of 3.8 kinesins/bead. *b*, average observed run lengths as a function of the average kinesin-bead ratio from the data in Fig. 2*b*. The average was calculated by dividing the total distance by the number of dissociations. *c*, average speed of the kinesin-coated beads as a function of the average kinesin-bead ratio. *Error bars* indicate S.E.

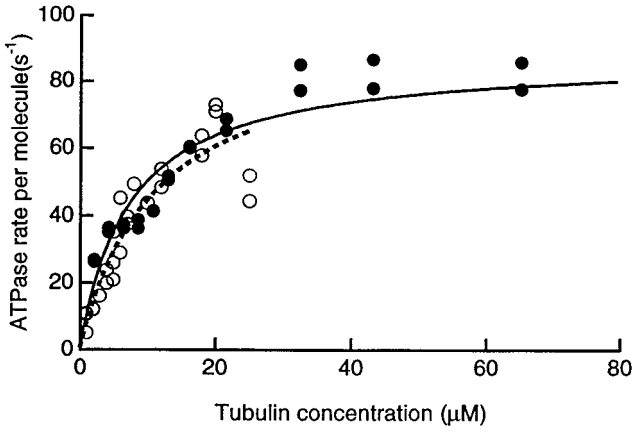

FIG. 4. **Steady-state microtubule-stimulated ATPase rate of recombinant heterotetrameric kinesin ($\alpha_2\beta_2$, *open circles*) and homodimeric kinesin (α_2, *closed circles*) adsorbed to 200-nm-diameter silica beads.** The *curves* are the least squares fits to the Michaelis-Menten equation with k_{cat} = 94 s^{-1} and K_m = 11 μM ($\alpha_2\beta_2$, *dotted line*) and k_{cat} = 88 s^{-1} and K_m = 7.4 μM (α_2, *solid line*).

therefore most of these runs are attributed to a single kinesin molecule. The mean run length of 1.2 μm was similar to that measured by Block *et al.* (9) using native squid kinesin. At the highest kinesin-bead ratio, 5.8, the average run length was greatest (Figs. 2*b* and 3*b*) due to an increase in the frequency of long runs. Presumably these long runs are due to two or more motors powering one bead; for two kinesin molecules to interact with the same microtubule at that density, we estimate that each kinesin must have a "reach" of about 25 nm.

The rate at which the beads attached to the microtubules increased as the average number of motors/bead increased (Fig. 3*a*). The attachment rate showed signs of saturation at the highest motor-bead ratio, such that the probability of a bead binding to a microtubule during a diffusive encounter at a kinesin-bead ratio of 4 is roughly half that of a bead saturated with kinesin. This indicates that a high proportion of the adsorbed motors are active, because otherwise there would be no saturation. This supports the radiometric assays described under "Experimental Procedures" showing that almost all the motors adsorbed to beads can bind to microtubules.

The speed at which beads moved along microtubules was independent of the kinesin-bead ratio (Fig. 3*c*), in agreement with earlier studies on bovine (8) and squid (9) kinesin. The mean speed was 882 ± 14 nm/s (mean ± S.E., n = 129) for this preparation at 25 °C.

ATPase Rate—The rate of ATP hydrolysis by kinesin bound to the 200-nm-diameter beads was measured using a modified malachite green assay. The kinesin-bead ratio was = 0.2, ensuring that greater than 90% of the beads with kinesin bound to them had only one kinesin molecule. The hydrolysis rate increased as the microtubule concentration was increased (Fig. 4), and the data were fitted with the Michaelis-Menten equation. For the $\alpha_2\beta_2$ preparation whose motility is characterized in Figs. 2 and 3, the maximal microtubule-stimulated hydrolysis rate was estimated to be 94 ± 13 s^{-1}/kinesin molecule (mean ± S.E.). The half-maximal hydrolysis rate occurred at a tubulin concentration of 11 ± 3 μM (mean ± S.E.). Similar results were obtained with other kinesin preparations including α_2 kinesin (Table I).

There are two ways that we might have underestimated the ATPase rate. First, if a bead has two (or more) motors on it, both motors may not be fully activated. At a kinesin-bead ratio of 0.2, ~10% of kinesin-beads possess multiple kinesin molecules. To determine whether multiple molecules on a bead are each activated to the same extent as a single kinesin molecule bound to single bead, the kinesin-bead ratio was increased 10-fold and the ATP hydrolysis rate/kinesin molecule was measured. At a kinesin-bead ratio of 2.0, 86% of kinesin molecules are bound to beads possessing at least one other kinesin molecule; the ATP hydrolysis rate/kinesin at 10 μM tubulin of 32 ± 1 s^{-1} was identical to the rate at a kinesin-bead ratio of 0.2, 32 ± 1 s^{-1}, indicating that several kinesin molecules on a single bead can be fully activated by microtubules.

A second way that the ATPase rate might be underestimated is if, over the course of an ATP hydrolysis assay, the depletion of ATP and the accumulation of ADP slow down the hydrolysis reaction. To minimize this effect, no more than 5% of the ATP was hydrolyzed during the course of our experiments. To estimate what effect the accumulation of a low concentration of ADP had on the measured hydrolysis rates, we assayed microtubule gliding speeds and ATPase rates in the presence of ADP. At 10% ADP ([ATP] = 0.9 mM, [ADP] = 0.1 mM), the microtubule gliding speed was reduced 13% from 610 ± 10 nm/s (n = 75) to 530 ± 10 nm/s (n = 75). The corresponding ATP hydrolysis rate at ~8 μM tubulin in the absence of beads was reduced 34% from 10.1 ± 0.4 s^{-1} to 6.7 ± 0.3 s^{-1}. These results suggest that the ADP accumulation decreases the instantaneous kinesin hydrolysis rate in two ways: by decreasing the rate at which kinesin moves along a microtubule and also by decreasing its apparent affinity for microtubules. The calculation of kinesin fuel economy and stoichiometry were corrected for this effect (see the legend to Table I).

Kinesin Fuel Economy and Stoichiometry—Dividing the speed of kinesin adsorbed to a silica bead by its maximum microtubule-stimulated hydrolysis rate yields an average fuel economy of 9.4 ± 1.3 and 9.9 ± 1.9 nm/ATP for the two prep-

arations containing light chains and 8.7 ± 0.7 nm/ATP for the preparation lacking light chains (Table I). Based on our controls, we expect the fuel economies to be overestimated by ~3%, due to the build-up of ADP in the ATPase assay but not in the motility assay. Correcting for this overestimate and dividing by the step size of 8.1 nm gives an average stoichiometry of 1.08 ± 0.09 steps/ATP hydrolyzed (data from the three preparations weighted by the reciprocals of their variances). The error is based on the uncertainties in the speed, the ATPase rate, the kinesin concentration measured using the radionucleotide assay, and the uncertainties of temperatures in the motility and ATPase assays (see the legend to Table I).

Our estimate of the stoichiometry depends crucially on the measurement of the specific activity of the kinesin enzyme. In this study, the concentration of active kinesin was measured as the number of sites that can exchange radioactively labeled ATP with unlabeled nucleotide divided by two because each kinesin molecule has two heads. We showed that adsorbing kinesin to the silica beads did not affect the concentration of active enzyme. Furthermore, almost all of the kinesin adsorbed to the beads with a geometry favorable for binding microtubules: 86% of the adsorbed motors were stimulated by microtubules to release their bound nucleotide ("Experimental Procedures."). Therefore, even though the adsorption of kinesin to the beads is nonspecific, a large fraction of the enzyme remains active with respect to nucleotide exchange and microtubule binding. A potential caveat to using nucleotide exchange to assay activity is that the time scale of exchange is minutes, whereas the time scale of the motility assay is seconds, the duration of the runs that the kinesin-coated beads make along the microtubules. It remains formally possible, therefore, that kinesin might switch between an active motile state and a quiescent immotile state on the time scale of tens of seconds. If this were the case, the quiescent state would be short lived enough that there would still be full exchange of nucleotide; as a result the measured ATPase rate would underestimate the true ATPase rate of the active motile enzyme, and the stoichiometry would be overestimated. However, a number of arguments show that the fraction of motors in such a quiescent state is small. First, if the quiescent state were an attached state, then we would have observed kinesin-coated beads binding to the microtubules for several seconds without moving. But this was not seen (less than 1% of beads failed to move continuously). On the other hand, if the quiescent state were a detached state, then we would expect that only the nonquiescent fraction of the motors would be attached to the microtubules even at very high tubulin concentrations. When the motors are attached to beads as in our assays, this is difficult to test. However, Hackney (31) used centrifugation assays on two-headed *Drosophila* kinesin in solution to show that the microtubule concentration required for activating the ATPase is identical to that required for binding. In other words, at high tubulin concentration all the motors are bound to the microtubules, ruling out the possibility of significant population of a quiescent, detached state.

DISCUSSION

By dividing the speed of movement of silica beads moving under the influence of single kinesin molecules by the ATP hydrolysis rate of the same beads under the same experimental conditions, we have shown that kinesin makes on average 1.08 ± 0.09 (mean ± S.E.) 8-nm steps for each molecule of ATP that it hydrolyzes. This is consistent with a stoichiometry of 1. Because our measurements were made on an ensemble of motors, we cannot discern whether kinesin takes one step after hydrolyzing one ATP molecule (1:1 coupling) or whether kinesin takes two consecutive steps after hydrolyzing two ATPs (2:2 coupling). In either case, one 8-nm step is produced per ATP hydrolyzed. However, mechanical measurements of single molecules at rate-limiting ATP concentrations (5, 14, 24) show that there are not clusters of 8-nm steps as would be expected if the coupling were 2:2 or some higher multiple. Therefore, taking our chemical data together with the mechanical recordings, we conclude that the coupling is 1:1, *i.e.* one ATP hydrolysis cycle results in a single step along a microtubule.

Under the low load conditions used in these experiments, the coupling between motility and ATP hydrolysis is tight; a stoichiometry of 1.08 ± 0.09 means that at least 90% of the hydrolysis cycles produce a mechanical step ($0.90 = 1.08 - 2 \times 0.09$ = mean − 2 × S.E.). The load in these assays is very small; the drag force associated with pulling a 200-nm diameter bead at 1 μm/s is only ~0.002 pN (32), which is <0.1% of the maximum force of ~6 pN that a kinesin molecule can generate (10–12). Whether the coupling remains tight at high load is not known.

A stoichiometry of 1 is consistent with the power stroke model and other models that propose a unitary coupling between the chemical and mechanical cycles of a motor (*e.g.* Refs. 23, 33, and 34). Our results rule out any model of chemomechanical transduction that requires two or more ATP/step ($n \leq 0.5$), such as the thermal ratchet models discussed in the Introduction. It also rules out other models mentioned that propose multiple steps powered from by single ATP ($n \geq 2$).

Acknowledgments—We thank Drs. A. Gordon, W. Hancock, B. Hille, and L. Wordeman for comments on an earlier version of the manuscript.

REFERENCES

1. Coy, D. L. & Howard, J. (1994) *Curr. Opin. Neurobiol.* **4,** 662–667
2. Bloom, G. S. & Endow, S. A. (1995) *Protein Profile* **2,** 1109–1171
3. Howard, J. (1996) *Annu. Rev. Physiol.* **58,** 703–729
4. Svoboda, K., Schmidt, C. F., Schnapp, B. J. & Block, S. M. (1993) *Nature* **365,** 721–727
5. Kojima, H., Muta, E., Higuchi, H. & Yanagida, T. (1997) *Biophys. J.* **73,** 2012–2022
6. Ray, S., Meyhöfer, E., Milligan, R. A. & Howard, J. (1993) *J. Cell Biol.* **121,** 1083–1093
7. Huang, T.-G., Suhan, J. & Hackney, D. D. (1994) *J. Biol. Chem.* **269,** 16502–16507
8. Howard, J., Hudspeth, A. J. & Vale, R. D. (1989) *Nature* **342,** 154–158
9. Block, S. M., Goldstein, L. S. B. & Schnapp, B. J. (1990) *Nature* **348,** 284–285
10. Hunt, A. J., Gittes, F. & Howard, J. (1994) *Biophys. J.* **67,** 766–781
11. Svoboda, K. & Block, S. M. (1994) *Cell* **77,** 773–784
12. Meyhöfer, E. & Howard, J. (1995) *Proc. Natl. Acad. Sci. U. S. A.* **92,** 574–578
13. Brady, S. T. (1985) *Nature* **317,** 73–75
14. Schnitzer, M. J. & Block, S. M. (1997) *Nature* **388,** 386–390
15. Lasek, R. J. & Brady, S. T. (1985) *Nature* **316,** 645–647
16. Cohn, S. A., Ingold, A. L. & Scholey, J. M. (1987) *Nature* **328,** 160–163
17. Astumian, R. D. & Bier, M. (1996) *Biophys. J.* **70,** 637–653
18. Rousselet, J., Salome, L., Ajdari, A. & Prost, J. (1994) *Nature* **370,** 446–448
19. Huxley, A. F. & Simmons, R. M. (1971) *Nature* **233,** 533–538
20. Lombardi, V., Piazzesi, G. & Linari, M. (1992) *Nature* **355,** 638–641
21. Yanagida, T., Arata, T. & Oosawa, F. (1985) *Nature* **316,** 366–369
22. Higuchi, H. & Goldman, Y. E. (1991) *Nature* **352,** 352–354
23. Howard, J. (1997) *Nature* **389,** 561–567
24. Hua, W., Young, E. C., Fleming, M. L. & Gelles, J. (1997) *Nature* **388,** 390–393
25. Hyman, A. A., Chretién, D., Arnal, I. & Wade, R. H. (1995) *J. Cell Biol.* **128,** 117–125
26. Saxton, W. M., Porter, M. E., Cohn, S. A., Scholey, J. M., Raff, E. C. & McIntosh, J. R. (1988) *Proc. Natl. Acad. Sci. U. S. A.* **85,** 1109–1113
27. Stewart, R. J., Thaler, J. P. & Goldstein, L. S. B. (1993) *Proc. Natl. Acad. Sci. U. S. A.* **90,** 5209–5213
28. Hackney, D. D., Levitt, J. D. & Suhan, J. (1992) *J. Biol. Chem.* **267,** 8696–8701
29. Mickey, B. & Howard, J. (1994) *J. Cell Biol.* **130,** 909–917
30. Howard, J., Hunt, A. J. & Baek, S. (1993) *Methods Cell Biol.* **39,** 138–147
31. Hackney, D. D. (1994) *J. Biol. Chem.* **269,** 16508–16511
32. Berg, H. C. (1983) *Random Walks in Biology*, p. 56, Princeton University Press, Princeton, NJ
33. Lymn, R. W. & Taylor, E. W. (1971) *Biochemistry* **10,** 4617–4624
34. Eisenberg E. & Hill T. L. (1978) *Prog. Biophys. Mol. Biol.* **33,** 55–82